Optimal Control of Sensor Threshold for Autonomous Wide Area Search Munitions

Brian A. Kish,[*] David R. Jacques,[†] and Meir Pachter[‡]

Air Force Institute of Technology

2950 Hobson Way, Wright Patterson AFB, OH, 45433, USA

The optimal employment of autonomous wide area search munitions is addressed. The scenario considered involves an airborne munition searching a battle space for stationary targets in the presence of false targets. Targets are modelled with uniform, Poisson, and normal distributions. False targets are modelled with Poisson distributions. All relevant parameters can be extracted from intelligence information on the enemy's order of battle and the sensor performance specification. Analytic weapon effectiveness measures are derived using applied probability theory. The effectiveness measures derived in this paper handle time-varying parameters which characterize the battle space environment and the performance of the munition's sensor. This allows the formulation and solution of optimization problems that maximize the probability of a target attack while at the same time constraining the probability of a false target attack. Optimal schedules for controlling the sensor threshold during the flight are derived and compared to the optimal constant-threshold results. An increase in weapon effectiveness is demonstrated when the sensor threshold is dynamically controlled during the flight.

---

[*]Major, United States Air Force, AIAA Senior Member.
[†]Assistant Professor, Department of Aeronautical Engineering, AIAA Senior Member.
[‡]Professor, Department of Electrical Engineering, AIAA Associate Fellow.

Report Documentation Page

1. REPORT DATE **AUG 2005**	2. REPORT TYPE	3. DATES COVERED **00-00-2005 to 00-00-2005**
4. TITLE AND SUBTITLE **Optimal Control of Sensor Threshold for Autonomous Wide Area Search Munitions**		5a. CONTRACT NUMBER
		5b. GRANT NUMBER
		5c. PROGRAM ELEMENT NUMBER
6. AUTHOR(S)		5d. PROJECT NUMBER
		5e. TASK NUMBER
		5f. WORK UNIT NUMBER
7. PERFORMING ORGANIZATION NAME(S) AND ADDRESS(ES) **Air Force Research Laboratory,Air Vehicles Directorate,Wright Patterson AFB,OH,45433**		8. PERFORMING ORGANIZATION REPORT NUMBER
9. SPONSORING/MONITORING AGENCY NAME(S) AND ADDRESS(ES)		10. SPONSOR/MONITOR'S ACRONYM(S)
		11. SPONSOR/MONITOR'S REPORT NUMBER(S)
12. DISTRIBUTION/AVAILABILITY STATEMENT **Approved for public release; distribution unlimited**		
13. SUPPLEMENTARY NOTES		
14. ABSTRACT		
15. SUBJECT TERMS		

| 16. SECURITY CLASSIFICATION OF:			17. LIMITATION OF ABSTRACT	18. NUMBER OF PAGES	19a. NAME OF RESPONSIBLE PERSON
a. REPORT **unclassified**	b. ABSTRACT **unclassified**	c. THIS PAGE **unclassified**		**30**	

Nomenclature

c Receiver Operating Characteristic Curve Parameter

$\mathcal{C}$ Events involving Classified Encounters

$\mathcal{E}$ Events involving Encounters

H Hamiltonian

L Integrand of Cost Functional

P_{FTA} Probability of a False Target Attack

P_{FTE} Probability of a False Target Encounter

P_{FTR} Probability of a False Target Report

P_{TA} Probability of a Target Attack

P_{TE} Probability of a Target Encounter

P_{TR} Probability of a Target Report

r Search Radius

R Terminal Radius

t Time

T Mission Duration

v Velocity

w Swath Width

x Dynamic Poisson Parameter

y Probability of a Target Attack when no False Targets exist

z Probability of a False Target Attack

α False Target Density

β Target Density

λ Costate

μ Rate of Encounters

ρ Radius

σ Standard Deviation

τ Time

I. Introduction

Several types of autonomous wide area search munitions are currently being developed for high risk air-to-ground missions. These airborne munitions will deploy to a battle space and autonomously search, detect, classify, and attack targets. In this paper, the presence of false targets in the battle space is acknowledged up front and analytic weapon effectiveness measures are derived based on target and false target probability distributions as well as the munition's sensor characteristics. All relevant parameters can be extracted from intelligence information on the enemy's order of battle and the sensor performance specification. This has been done for wide area search munitions in the past; however, the problem parameters were assumed constant.[3] The results of Ref. 3 are now generalized to handle time-varying parameters. This then allows one to address the optimal control of the sensor threshold to maximize the probability of a target attack without unduly increasing the probability of a false target attack. The latter is crucial for making autonomous operation acceptable to the war fighter.

The battle space geometries considered are rectangular and circular. In a rectangular battle space of length l and width w, the munition covers the area using a constant velocity v starting at initial time $t = 0$ and ending at final time $t = T$. The sensor footprint is rectangular with swath width w and incremental swath length vdt as shown in Figure 1(a). Hence, the munition covers the battle space in one sweep. In a circular battle space of radius R, the munition covers the area using concentric annuli of thickness dr as shown in Figure 1(b). The munition starts at the origin and progresses outward. This method of concentric annuli approximates an outward spiral search pattern.

(a) Rectangular Battle Space   (b) Circular Battle Space
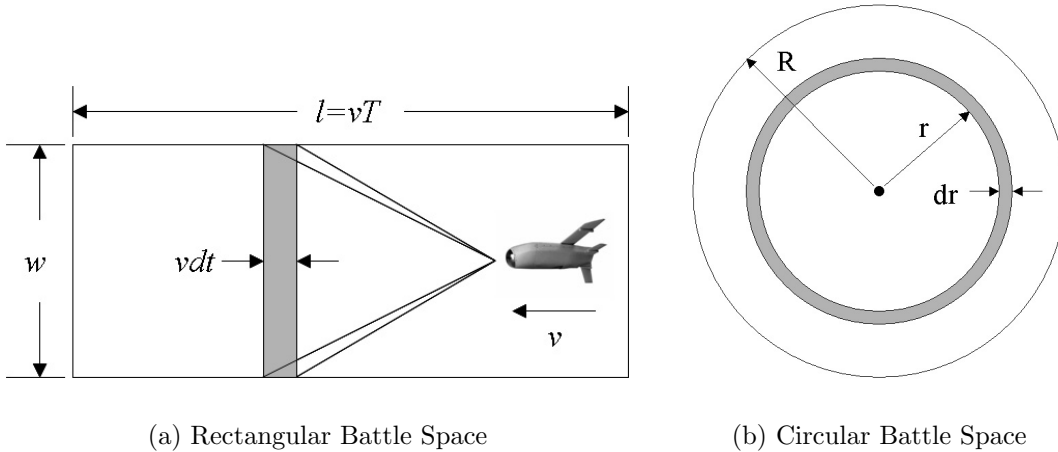
Figure 1. Battle Space Geometries

The scenarios considered involve one munition searching for stationary targets among a field of false targets. In operations research, the distribution of false targets in a battle space is often modelled using a Poisson distribution.[1–3] Three such scenarios involving a Poisson field of false targets are examined. The first scenario addresses the case when a single target may appear anywhere within a rectangular battle space with equal probability, thus the target encounter is modelled with a uniform distribution. The second scenario addresses the case when target encounters occur at an expected rate in a rectangular battle space, thus target encounters are modelled with a Poisson distribution. Finally, the third scenario addresses the case when specific information is available about a target (i.e., position coordinates with some error). The target is modelled with a circular-normal distribution and the corresponding battle space is defined as circular. In all three scenarios, flight altitude and speed are constant, and the munition covers the entire search area.

A.   Sensor Performance

When a sensor encounters an object, it compares the image to a stored template or pattern and either declares the object a target or a false target. In practice, detected objects are classified to a certain level of discrimination. For example, one may classify on object as either air breathing or ballistic. A finer level of discrimination may be a specific type of air-breathing or ballistic object. Regardless of the level of discrimination, there is a point where the sensor reports a detected object as either a target thereby authorizing an attack, or a false target thereby commanding no attack. Sensor performance is judged by how often the sensor is correct. The probability of a target report, P_{TR}, is the probability the sensor correctly reports a *target* when a *target* is encountered. The probability of a false target report, P_{FTR}, is the probability the sensor correctly reports a *false target* when a *false target* is encountered. Together, P_{TR} and P_{FTR} determine the entries of the binary "confusion matrix" shown in Table 1 which can be used to determine the outcome of a random draw each time an object is encountered in simulation.

Table 1.   Confusion Matrix

	Encountered Object	
	Target	False Target
Declared Object		
Target	P_{TR}	$1 - P_{FTR}$
False Target	$1 - P_{TR}$	P_{FTR}

The expression $(1 - P_{TR})$ represents the probability the sensor reports a *false target* when a *target* is encountered. This type of error results in a target not being attacked.

The expression $(1 - P_{FTR})$ represents the probability the sensor reports a *target* when a *false target* is encountered. This type of error results in a false target being attacked. For this binary confusion matrix, true positive fraction is P_{TR}, and false positive fraction is $(1 - P_{FTR})$. A Receiver Operating Characteristic (ROC) curve is a plot of true positive fraction versus false positive fraction that starts at $(0,0)$, then monotonically increases to $(1,1)$. The ROC curve model adapted from Ref. 4 is used:

$$(1 - P_{FTR}) = \frac{P_{TR}}{(1 - c) P_{TR} + c} \tag{1}$$

where the non-dimensional scalar parameter, $c \in [1, \infty)$, depends on the sensor and data processing algorithm. It also depends on the munition speed (dwell time), and engagement geometry, which includes flight altitude and look angle. A family of ROC curves parame-
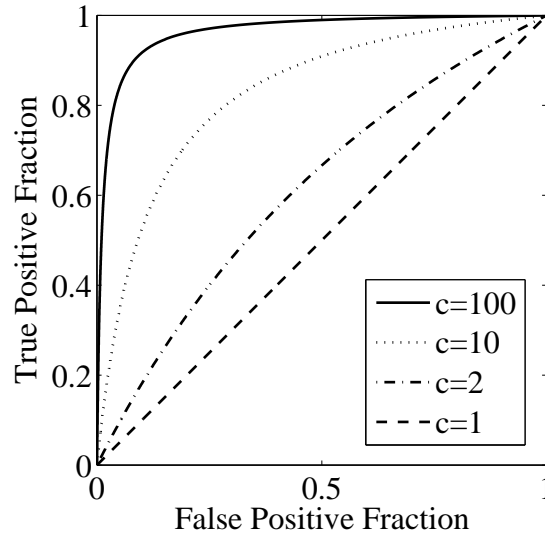
Figure 2. Family of ROC Curves.

terized by c is shown in Figure 2. As c increases, the ROC improves. As $c \to \infty$, the area under the curve approaches unity indicating perfect identification. For all examples in this paper, the ROC parameter will be $c = 100$.

The operating point on a ROC curve is the ordered pair $[P_{TR}, (1 - P_{FTR})]$. For a given sensor and algorithm, the operating point is determined by the sensor's threshold. Setting the threshold is tantamount to setting P_{TR}. The value for $(1 - P_{FTR})$ is calculated using Eq. (1). Given a ROC curve, the goal is finding the optimal P_{TR} – either constant, or as a function of time or space.

B. Optimal Control Problem Formulation

An operator wants the probability of a target attack, P_{TA}, in a battle space to be high and the probability of a false target attack, P_{FTA}, to be low. Therefore, P_{TA} and P_{FTA} become weapon effectiveness measures. Unfortunately, increasing P_{TR} by reducing sensor threshold with a view to *increase* P_{TA} also increases $(1 - P_{FTR})$ and consequently P_{FTA}. This state of affairs is modelled by the ROC. Thus, the operator's objectives are competing, and a trade-off situation arises. To ensure P_{FTA} stays low, a constraint is imposed on it. The optimization problem statement is then

$$\text{Maximize:} \quad P_{TA}$$
$$\text{Subject to:} \quad P_{FTA} \leq P_{FTA_{max}}$$

where $P_{FTA_{max}}$ is set by the designer or mission planner.

To solve the posed optimization problem, expressions are developed for P_{TA} and P_{FTA} for the considered scenarios. This involves integrating probability density functions parameterized by P_{TR}, velocity, and search width, as well as data on the battle space environment concerning target and false target densities. The latter are obtained from knowledge of the order of battle. Velocity and search width are assumed constant, so the decision variable is P_{TR}. The explicit ROC model given by Eq. (1) is used; however, the discerned trends will apply to any ROC. With an inequality constraint, the unconstrained problem is solved first to see if the constraint is met. If $P_{FTA} < P_{FTA_{max}}$, the unconstrained solution is used. Otherwise the constraint is active and the constrained problem is solved with an equality constraint. Since the decision variable P_{TR} is a probability, it is bounded by $[0, 1]$.

To provide a benchmark, constant-threshold problems are solved first. Holding P_{TR} constant yields a static (parameter) optimization problem and closed-form solutions are possible. More importantly from an operational point of view, using a constant sensor threshold (i.e. a constant P_{TR}) is the easiest way to employ a wide area search munition. The dynamic-threshold problem and consequently the dynamic-P_{TR} problem can be formulated as a text book optimal control problem.[5,6]

II. Scenario 1: One Uniformly-Distributed Target and a Poisson Field of False Targets

The scenario when one target is uniformly distributed over a battle space among a Poisson field of false targets is considered. With an expendable munition, the probability of an attack occurring during the time interval $[t, t + dt]$ is conditioned on the probability of no attacks occurring prior to t. The probabilities in Ref. 3 were calculated assuming constant parameters. The probabilities are re-derived for time-varying parameters.

In the infinitesimal interval $[t, t + dt]$, like that shown in Figure 1(a), three events can occur: a target is attacked, a false target is attacked, or an attack does not occur. Assuming no attacks occurred prior to t, the probability of a target attack occurring in the time interval $[t, t + dt]$ is

$$P_{TR}(t) \cdot P_{TE}(t) \tag{2}$$

where $P_{TE}(t)$ is the probability of a target encounter in the infinitesimal footprint. Similarly, the probability of a false target attack is

$$[1 - P_{FTR}(t)] \cdot P_{FTE}(t) \tag{3}$$

where $P_{FTE}(t)$ is the probability of a false target encounter in the infinitesimal footprint. Finally, the probability of no attack occurring during $[t, t + dt]$ is

$$[1 - P_{TR}(t)] \cdot P_{TE}(t) + P_{FTR}(t) \cdot P_{FTE}(t). \tag{4}$$

The classification probabilities, $P_{TR}(t)$, $1 - P_{TR}(t)$, $P_{FTR}(t)$, and $1 - P_{FTR}(t)$, are specified. The encounter probabilities, $P_{TE}(t)$ and $P_{FTE}(t)$, are determined from the respective target and false target distributions. For one uniformly-distributed target,

$$P_{TE}(t) = \frac{w(t) \, v(t) \, dt}{A_s} \tag{5}$$

where the battle space or area searched, A_s, is

$$A_s \equiv \int_0^T w(t) \, v(t) \, dt. \tag{6}$$

For a Poisson field of false targets,

$$P_{FTE}(t) = \alpha(t) \, w(t) \, v(t) \, dt \tag{7}$$

where $\alpha(t)$ is the mean false target density at time t. Indeed, the false target density in the battle space need not be constant and could vary from place to place thereby being time dependent.

Formulae for the probabilities of no previous attacks prior to t are now given. Detailed derivations are given in the Appendix. For one uniformly-distributed target, the probability of no target attack occurring prior to time t is

$$P_{\overline{TA}}(t) = 1 - \frac{1}{A_s} \int_0^t P_{TR}(\tau) \, w(\tau) \, v(\tau) \, d\tau. \tag{8}$$

For a Poisson field of false targets with density $\alpha(\tau)$, $0 \leq \tau \leq t$, the probability of no false target attacks occurring prior to time t is

$$P_{\overline{FTA}}(t) = e^{-\int_0^t [1-P_{FTR}(\tau)]\alpha(\tau)w(\tau)v(\tau)d\tau} \tag{9}$$

The probability of a target attack can now be calculated as

$$
\begin{aligned}
P_{TA} &= \int_0^T P_{TR}(t) \cdot P_{TE}(t) \cdot P_{\overline{FTA}}(t) \\
&= \int_0^T \frac{1}{A_s} P_{TR}(t) \, w(t) \, v(t) \, e^{-\int_0^t [1-P_{FTR}(\tau)]\alpha(\tau)w(\tau)v(\tau)d\tau} dt
\end{aligned}
\tag{10}
$$

and the probability of a false target is

$$
\begin{aligned}
P_{FTA} &= \int_0^T [1 - P_{FTR}(t)] \cdot P_{FTE}(t) \cdot P_{\overline{TA}}(t) \cdot P_{\overline{FTA}}(t) \\
&= \int_0^T [1 - P_{FTR}(t)] \, \alpha(t) \, w(t) \, v(t) \times \\
&\quad \left(1 - \int_0^t \frac{1}{A_s} P_{TR}(\tau) \, w(\tau) \, v(\tau) \, d\tau\right) e^{-\int_0^t [1-P_{FTR}(\tau)]\alpha(\tau)w(\tau)v(\tau)d\tau} dt.
\end{aligned}
\tag{11}
$$

The problem of finding the optimal $P_{TR}(t)$, $0 \leq t \leq T$, assuming w, v, and α are constant is now addressed. Recall $[1 - P_{FTR}(t)]$ is determined from $P_{TR}(t)$, because they are related by the ROC.

A. Constant-Threshold

When the sensor threshold is constant during the flight, P_{TR} and consequently P_{FTR} are constant, and closed-form solutions are obtained when evaluating the integrals in Eq. (10) and Eq. (11). The probability of a target attack is

$$P_{TA} = P_{TR} \frac{1 - e^{-(1-P_{FTR})\alpha wvT}}{(1 - P_{FTR})\,\alpha wvT} \tag{12}$$

and the probability of a false target attack is

$$P_{FTA} = 1 - P_{TA} - (1 - P_{TR}) \, e^{-(1-P_{FTR})\alpha wvT}. \tag{13}$$

The ROC model in Eq. (1) is invoked to reduce the problem to a one-dimensional search for P_{TR}^*. The goal is maximizing P_{TA} subject to $P_{FTA} \leq P_{FTA_{max}}$.

To show an example, values are needed for the constants c, w, v, α, and T. Units are time units. Assuming $c = 100$, $\alpha wv = 50$ [1/time] and $T = 0.5$ [time], the outcome probabilities

are plotted versus P_{TR}. Figure 3 shows the best unconstrained solution is $P^*_{TR_u} = 0.723$ with a corresponding $P^*_{TA_u} = 0.535$ and $P^*_{FTA_u} = 0.318$. The subscript u is used to denote unconstrained solutions. If P_{FTA} is bounded by $P_{FTA_{max}} = 0.2$, the best constrained solution is $P^*_{TR} = 0.563$ with a corresponding $P^*_{TA} = 0.483$. In Figure 3, the outcome probability functions are smooth and well-behaved. The function for P_{TA} has only one peak and never crosses the line where $P_{TA} = P_{TR}$. The function for P_{FTA} is monotonically increasing in P_{TR}, so any constrained solution will be unique. Finally, the function for the probability of no attack occurring is monotonically decreasing in P_{TR} as expected.
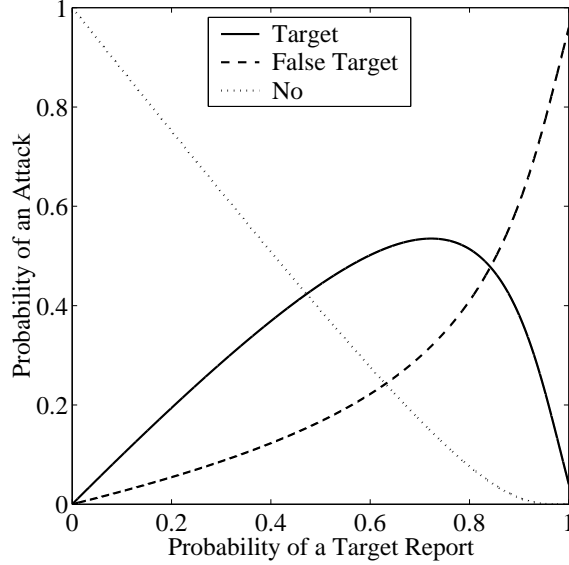
Figure 3. Outcome probabilities versus probability of a target report. The scenario involves one uniformly-distributed target among a Poisson field of false targets. Probability of a target report is constant throughout the flight, $c = 100$, $\alpha wv = 50$ [1/time], and $T = 0.5$ [time].

The constant-threshold optimization problem can be solved for a number of $P_{FTA_{max}}$ values and a plot of P^*_{TR} versus $P_{FTA_{max}}$ can be generated. Figure 4 illustrates the sensitivity of the solution to changes in the upper bound $P_{FTA_{max}}$. For $P_{FTA_{max}} > 0.32$, the unconstrained solution is used.
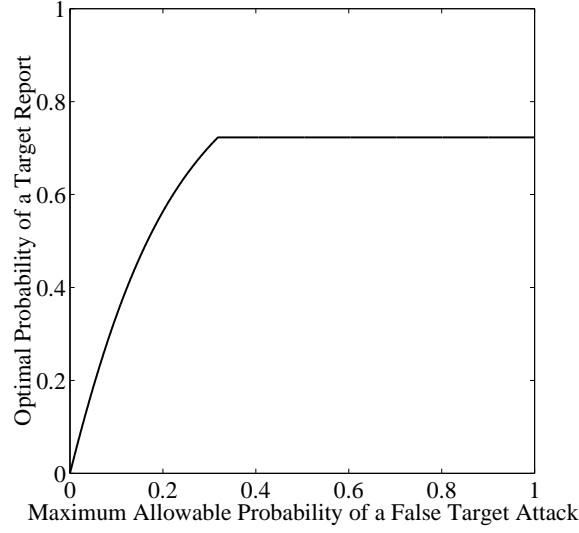
Figure 4. Optimal probability of a target report versus maximum allowable probability of a false target attack. The scenario involves one uniformly-distributed target among a Poisson field of false targets. Probability of a target report is constant throughout the flight, $c = 100$, $\alpha wv = 50$ [1/time], and $T = 0.5$ [time].

B. Dynamic-Threshold

When P_{TR}, and consequently P_{FTR}, are dynamic, an optimal control problem is on hand. The state variables become

$$x = \int_0^t \alpha wv \left[1 - P_{FTR}(\tau)\right] d\tau \tag{14}$$

$$y = \int_0^t \frac{1}{T} P_{TR}(\tau) d\tau \tag{15}$$

$$z = \int_0^t \alpha wv \left[1 - P_{FTR}(\tau)\right] \left[1 - y(\tau)\right] e^{-x(\tau)} d\tau \tag{16}$$

and the cost functional integrand, L, is

$$L = -\frac{1}{T} P_{TR}(t) e^{-x(t)}. \tag{17}$$

Obviously,

$$P_{TA} = -\int_0^T L\left[P_{TR}(t), x(t)\right] dt. \tag{18}$$

The states equations are

$$\dot{x} = \alpha w v \left[1 - P_{FTR}(t)\right] \tag{19}$$

$$\dot{y} = \frac{1}{T} P_{TR}(t) \tag{20}$$

$$\dot{z} = \alpha w v \left[1 - P_{FTR}(t)\right] \left[1 - y(t)\right] e^{-x(t)} \tag{21}$$

After applying Eq. (1) for the ROC model, the Hamiltonian, H, becomes

$$H = \left(\lambda_y - e^{-x}\right) \frac{1}{T} P_{TR} + \alpha w v \frac{P_{TR}}{(1-c) P_{TR} + c} \left[\lambda_x + \lambda_z (1-y) e^{-x}\right] \tag{22}$$

and the costate differential equations become

$$\dot{\lambda}_x = \lambda_z \alpha w v \frac{P_{TR}}{(1-c) P_{TR} + c} (1-y) e^{-x} - \frac{1}{T} P_{TR} e^{-x} \tag{23}$$

$$\dot{\lambda}_y = \lambda_z \alpha w v \frac{P_{TR}}{(1-c) P_{TR} + c} e^{-x} \tag{24}$$

$$\dot{\lambda}_z = 0 \tag{25}$$

Taking the partial derivative of H with respect to the decision variable P_{TR} gives

$$\frac{\partial H}{\partial P_{TR}} = \left(\lambda_y - e^{-x}\right) \frac{1}{T} + \frac{\left[\lambda_x + \lambda_z (1-y) e^{-x}\right] \alpha w v c}{\left[(1-c) P_{TR} + c\right]^2} \tag{26}$$

Solving $\frac{\partial H}{\partial P_{TR}} = 0$, the optimal control is

$$P_{TR}^*(t) = \frac{c \pm \sqrt{\frac{\left\{\lambda_x(t) + \lambda_z [1 - y(t)] e^{-x(t)}\right\} \alpha w v c T}{\left[e^{-x(t)} - \lambda_y(t)\right]}}}{c - 1}. \tag{27}$$

Only the "minus" root is of interest, since the "plus" root puts P_{TR} outside of $[0, 1]$ for all time. One is also interested in the optimal unconstrained solution, $P_{TR_u}^*$, which is

$$P_{TR_u}^*(t) = \frac{c - \sqrt{\lambda_x(t) \alpha w v c T e^{x(t)}}}{c - 1}. \tag{28}$$

Taking the derivative of Eq. (28) with respect to t gives

$$\dot{P}_{TR_u}^*(t) = \sqrt{\frac{\alpha w v e^{-x(t)}}{4 c T \lambda_x(t)}} \left[P_{TR}^*(t)\right]^2 > 0. \tag{29}$$

Therefore, $P^*_{TR_u}$ is monotonically increasing. At the terminal point where $\lambda_x(T) = 0$, $P^*_{TR_u}(T) = \frac{c}{c-1} > 1$. Thus, the constraint $P_{TR} \in [0, 1]$ becomes active prior to the end and remains active until time T. This represents, for the unconstrained problem, a "go for broke" tactic in the end game.

Assuming $c = 100$, $\alpha w v = 50$ [1/time], and $T = 0.5$ [time], the constrained problem can be solved for a number of $P_{FTA_{max}}$ values. Figure 5 shows optimal solutions as a function of time for three values of $P_{FTA_{max}}$. As $P_{FTA_{max}}$ decreases, the optimal solution flattens out approaching a constant-threshold solution.
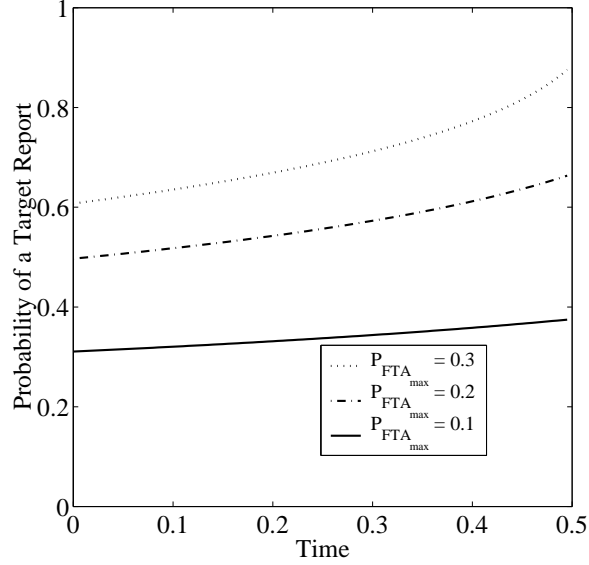
Figure 5.   Optimal probability of a target report versus time.   The scenario involves one uniformly-distributed target among a Poisson field of false targets. $c = 100$, $\alpha w v = 50$ **[1/time], and** $T = 0.5$ **[time].**

The objective function values of the dynamic solutions can be compared to those of the constant solutions. Figure 6 shows, for the assumed parameters, that the optimal dynamic solution is at most 3.4 percent better than the optimal constant solution. Depending on the application, this improvement may or may not be worth the added complexity.
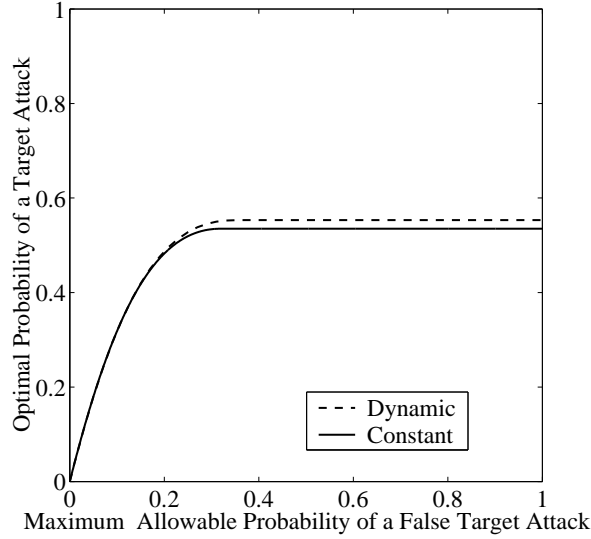
Figure 6. Optimal probability of a target attack versus maximum allowable probability of a false target attack. The scenario involves one uniformly-distributed target among a Poisson field of false targets. $c = 100$, $\alpha wv = 50$ **[1/time], and** $T = 0.5$ **[time].**

III. Scenario 2: Poisson Fields of Targets and False Targets

The scenario when targets are also modelled with a Poisson distribution is considered. For this scenario the battle space consists of a Poisson field of targets and a Poisson field of false targets. The derivation of probabilities is similar to the previous scenario with the following changes. For a Poisson field of targets,

$$P_{TE}(t) = \beta(t) w(t) v(t) dt \tag{30}$$

where $\beta(t)$ is the mean target density at time t. The probability of no target attacks occurring prior to time t is

$$P_{\overline{TA}}(t) = e^{-\int_0^t P_{TR}(\tau)\beta(\tau)w(\tau)v(\tau)d\tau}. \tag{31}$$

The probability of a target attack can now be calculated as

$$
\begin{aligned}
P_{TA} &= \int_0^T P_{TR}(t) \cdot P_{TE}(t) \cdot P_{\overline{TA}}(t) \cdot P_{\overline{FTA}}(t) \\
&= \int_0^T P_{TR}(t)\,\beta(t)\,w(t)\,v(t)\,e^{-\int_0^t \{[1-P_{FTR}(\tau)]\alpha(\tau)+P_{TR}(\tau)\beta(\tau)\}w(\tau)v(\tau)d\tau} dt
\end{aligned} \tag{32}
$$

and the probability of a false target attack is

$$
\begin{aligned}
P_{FTA} &= \int_0^T [1 - P_{FTR}(t)] \cdot P_{FTE}(t) \cdot P_{\overline{TA}}(t) \cdot P_{\overline{FTA}}(t) \\
&= \int_0^T [1 - P_{FTR}(t)] \, \alpha(t) \, w(t) \, v(t) \, e^{-\int_0^t \{[1-P_{FTR}(\tau)]\alpha(\tau)+P_{TR}(\tau)\beta(\tau)\}w(\tau)v(\tau)d\tau} dt \quad (33)
\end{aligned}
$$

The parameters w, v, α, and β are assumed constant.

A. Constant-Threshold

When P_{TR} and consequently P_{FTR} are constant, closed-form solutions are obtained when evaluating the integrals in Eq. (32) and Eq. (33). The probability of a target attack is

$$
P_{TA} = \frac{P_{TR}\beta}{(1 - P_{FTR})\,\alpha + P_{TR}\beta} \left\{ 1 - e^{-[(1-P_{FTR})\alpha+P_{TR}\beta]wvT} \right\} \tag{34}
$$

and the probability of a false target attack is

$$
P_{FTA} = 1 - P_{TA} - e^{-[(1-P_{FTR})\alpha+P_{TR}\beta]wvT} \tag{35}
$$

To show an example, values must be provided for the various constants. Units are time and distance units. Invoking the ROC model in Eq. (1) and assuming $c = 100$, $w = 0.2$ [distance], $v = 50$ [distance/time], $\alpha = 10$ [1/distance^2], $\beta = 1$ [1/distance^2], and $T = 0.5$ [time], the outcome probabilities are plotted versus P_{TR}. Figure 7 shows the best unconstrained solution is $P_{TR_u}^* = 0.513$ with a corresponding $P_{TA_u}^* = 0.793$ and $P_{FTA_u}^* = 0.161$. If P_{FTA} is bound by $P_{FTA_{max}} = 0.1$, the best constrained solution is $P_{TR}^* = 0.292$ with a corresponding $P_{TA}^* = 0.711$.

Like the previous scenario, the function for P_{TA} has only one peak. Unlike the previous scenario, the values of α and β can skew the function for P_{TA} above or below the line where $P_{TA} = P_{TR}$. However, the function for P_{FTA} is still monotonically increasing. Thus, any constrained solution will be unique.

B. Dynamic-Threshold

When P_{TR}, and consequently P_{FTR}, are dynamic, the state variables become

$$
x = \int_0^t \{ [1 - P_{FTR}(\tau)] \, \alpha + P_{TR}(\tau)\,\beta \} \, wv\,d\tau \tag{36}
$$

$$
z = \int_0^t [1 - P_{FTR}(\tau)] \, \alpha wv e^{-x(\tau)} d\tau \tag{37}
$$
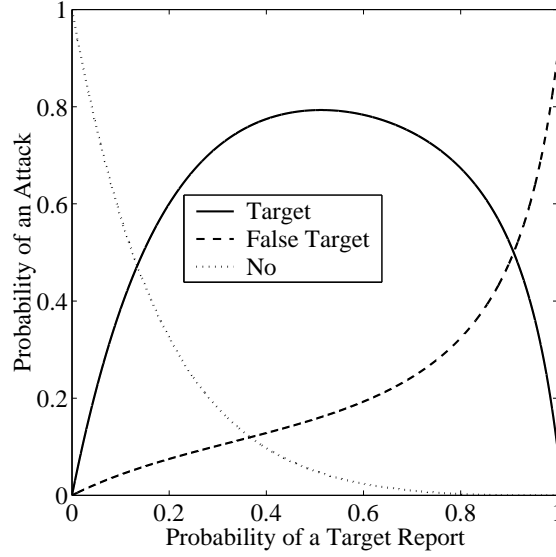
Figure 7. Outcome probabilities versus probability of a target report. The scenario involves a Poisson field of targets and a Poisson field of false targets. Probability of a target report is constant throughout the flight, $c = 100$, $w = 0.2$ **[distance],** $v = 50$ **[distance/time],** $\alpha = 10$ **[1/distance^2],** $\beta = 1$ **[1/distance^2], and** $T = 0.5$ **[time].**

and L is

$$L = -P_{TR}(t)\,\beta wv e^{-x(t)}. \tag{38}$$

Since both targets and false targets have Poisson distributions, the state x represents a combined dynamic Poisson parameter. Hence there is no need for a separate y state. The state equations are

$$\dot{x} = \{[1 - P_{FTR}(t)]\alpha + P_{TR}(t)\beta\}\,wv \tag{39}$$

$$\dot{z} = [1 - P_{FTR}(t)]\,\alpha wv e^{-x(t)} \tag{40}$$

After applying Eq. (1) for the ROC model, the Hamiltonian becomes

$$H = (\lambda_x - e^{-x})\,P_{TR}\beta wv + (\lambda_x + \lambda_z e^{-x})\,\alpha wv \frac{P_{TR}}{(1-c)\,P_{TR}+c} \tag{41}$$

and the costate differential equations become

$$\dot{\lambda}_x = \left[\lambda_z\alpha\frac{P_{TR}}{(1-c)\,P_{TR}+c} - P_{TR}\beta\right]wv e^{-x} \tag{42}$$

$$\dot{\lambda}_z = 0 \tag{43}$$

Taking the partial derivative of H with respect to the decision variable P_{TR} gives

$$\frac{\partial H}{\partial P_{TR}} = \left(\lambda_x - e^{-x}\right)\beta wv + \frac{\left(\lambda_x + \lambda_z e^{-x}\right)\alpha wvc}{\left[(1-c)\,P_{TR} + c\right]^2} \tag{44}$$

Solving $\frac{\partial H}{\partial P_{TR}} = 0$, the optimal control is

$$P_{TR}^*(t) = \frac{c \pm \sqrt{\dfrac{c\alpha\left[\lambda_x(t) + \lambda_z e^{-x(t)}\right]}{\beta\left[e^{-x(t)} - \lambda_x(t)\right[}}}{c-1} \tag{45}$$

which is real-valued only if $\left[e^{-x(t)} - \lambda_x(t)\right] > 0$. Once again, only the "minus" root is used. One is also interested in the optimal unconstrained solution, which is

$$P_{TR_u}^*(t) = \frac{c - \sqrt{\dfrac{c\alpha\lambda_x(t)}{\beta\left[e^{-x(t)} - \lambda_x(t)\right]}}}{c-1}. \tag{46}$$

Taking the derivative of Eq. (46) with respect to t gives

$$\dot{P}_{TR_u}^*(t) = \sqrt{\frac{(wv)^2\,\alpha\beta e^{-2x(t)}}{4c\lambda_x(t)\left[e^{-x(t)} - \lambda_x(t)\right]}}\,\left[P_{TR}^*(t)\right]^2 > 0. \tag{47}$$

Therefore, $P_{TR_u}^*$ is monotonically increasing and $P_{TR_u}^*(T) = \frac{c}{c-1} > 1$. Thus, the "go for broke" tactic appears again for this unconstrained problem.

Assuming $c = 100$, $w = 0.2$ [distance], $v = 50$ [distance/time], $\alpha = 10$ [1/distance^2], $\beta = 1$ [1/distance^2], and $T = 0.5$ [time], the constrained problem is solved for a number of $P_{FTA_{max}}$ values. Figure 8 shows optimal solutions as a function of time for three values of $P_{FTA_{max}}$. Once again, as $P_{FTA_{max}}$ decreases, the optimal solution flattens out approaching a constant-threshold solution.

The objective function values of the dynamic solutions are compared to those of the constant solutions. Figure 9 shows, for the assumed parameters, that the optimal dynamic solution is at most 3.6 percent better than the optimal constant solution. Depending on the application, this improvement may or may not be worth the added complexity. These first two scenarios involved constant ratios of targets to false targets, regardless of the sensor footprint position. The next scenario involves non-constant ratios of targets to false targets.
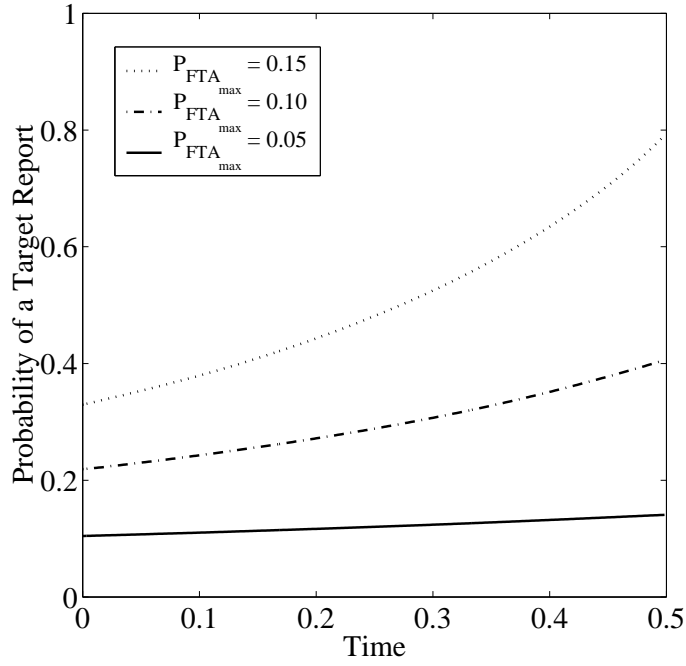
Figure 8. Optimal probability of a target report versus time. The scenario involves a Poisson field of targets and a Poisson field of false targets. $c = 100$, $w = 0.2$ [distance], $v = 50$ [distance/time], $\alpha = 10$ [1/distance^2], $\beta = 1$ [1/distance^2], and $T = 0.5$ [time].
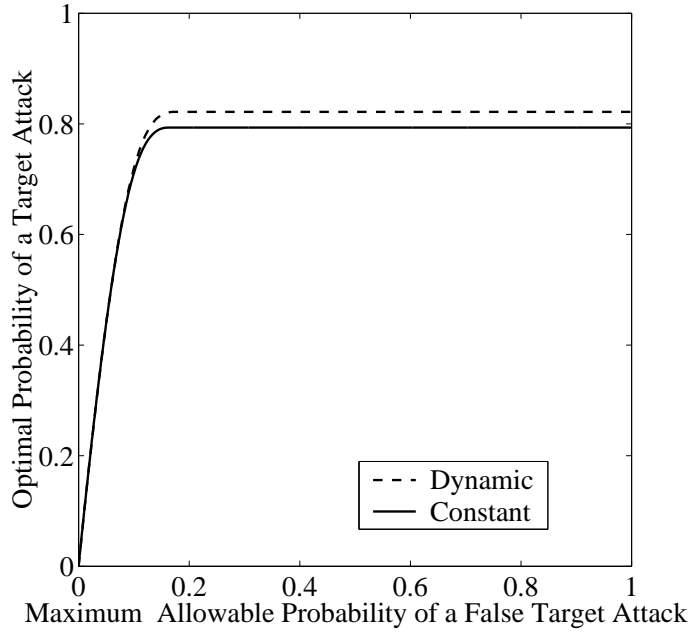

Figure 9. Optimal probability of a target attack versus maximum allowable probability of a false target attack. The scenario involves a Poisson field of targets and a Poisson field of false targets. $c = 100$, $w = 0.2$ [distance], $v = 50$ [distance/time], $\alpha = 10$ [1/distance^2], $\beta = 1$ [1/distance^2], and $T = 0.5$ [time].

IV. Scenario 3: One Normally-Distributed Target and a Poisson Field of False Targets

The scenario when one target is normally distributed over a circular battle space among a Poisson field of false targets is now considered. The ratio of targets to false targets depends on the sensor footprint position. The normal distribution is circular, centered at the origin with variance σ^2. The derivation of probabilities is similar to the first scenario with the following changes. For one normally-distributed target,

$$P_{TE}(r) = \frac{1}{2\pi\sigma^2} e^{-\frac{r^2}{2\sigma^2}} 2\pi r dr. \tag{48}$$

The probability of no false target attacks occurring prior to reaching radius r is

$$P_{\overline{FTA}}(r) = e^{-\int_0^r 2\pi[1-P_{FTR}(\rho)]\alpha(\rho)\rho d\rho}, \tag{49}$$

and the probability of no target attack occurring prior to reaching radius r is

$$P_{\overline{TA}}(r) = 1 - \int_0^r \frac{P_{TR}(\rho)}{\sigma^2} e^{-\frac{\rho^2}{2\sigma^2}} \rho d\rho. \tag{50}$$

The probability of a target attack can now be calculated as

$$
\begin{aligned}
P_{TA} &= \int_0^R P_{TR}(r) \cdot P_{TE}(r) \cdot P_{\overline{FTA}}(r) \\
&= \int_0^R P_{TR}(r) \frac{r}{\sigma^2} e^{-\frac{r^2}{2\sigma^2}} \cdot e^{-\int_0^r 2\pi[1-P_{FTR}(\rho)]\alpha(\rho)\rho d\rho} dr
\end{aligned} \tag{51}
$$

and the probability of a false target attack is

$$
\begin{aligned}
P_{FTA} &= \int_0^R [1-P_{FTR}(r)] \cdot P_{FTE}(r) \cdot P_{\overline{TA}}(r) \cdot P_{\overline{FTA}}(r) \\
&= \int_0^R [1-P_{FTR}(r)] 2\pi r\alpha(r) \times \\
&\quad \left[1 - \int_0^r P_{TR}(\rho) \frac{\rho}{\sigma^2} e^{-\frac{\rho^2}{2\sigma^2}} d\rho\right] e^{-\int_0^r 2\pi[1-P_{FTR}(\rho)]\alpha(\rho)\rho d\rho} dr.
\end{aligned} \tag{52}
$$

The parameter α is assumed constant.

A.   Constant-Threshold

If P_{TR} and consequently P_{FTR} are constant, closed-form solutions are obtained when evaluating the integrals in Eq. (51) and Eq. (52). The probability of a target attack is

$$P_{TA} = \frac{P_{TR}}{2\sigma^2 \left[(1 - P_{FTR})\,\alpha\pi + \frac{1}{2\sigma^2}\right]} \left(1 - e^{-\left[(1-P_{FTR})\alpha\pi + \frac{1}{2\sigma^2}\right]R^2}\right) \tag{53}$$

and the probability of a false target attack is

$$P_{FTA} = 1 - P_{TA} - \left(1 - P_{TR} + P_{TR}e^{\frac{-R^2}{2\sigma^2}}\right) e^{-(1-P_{FTR})\alpha\pi R^2} \tag{54}$$

To show an example, values must be provided for the various constants. Units are distance units. Invoking the ROC model in Eq. (1) and assuming $c = 100$, $\alpha = 5$ [1/distance^2], $\sigma^2 = 0.25$ [distance^2], and $R = 5$ [distance], the outcome probabilities are plotted versus P_{TR}. Figure 10 shows the best unconstrained solution is $P^*_{TR_u} = 0.788$ with a corresponding $P^*_{TA_u} = 0.615$ and $P^*_{FTA_u} = 0.385$. If P_{FTA} is bound by $P_{FTA_{max}} = 0.20$, the best constrained solution is $P^*_{TR} = 0.057$ with a corresponding $P^*_{TA} = 0.057$. This is a significant reduction in performance.
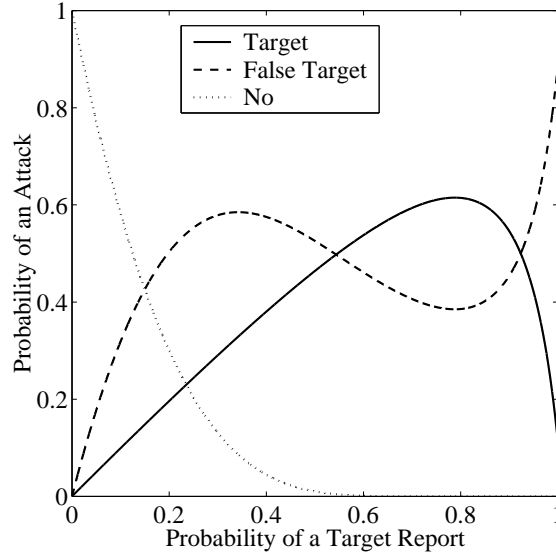
Figure 10. Outcome probabilities versus probability of a target report. The scenario involves a normally-distributed target and a Poisson field of false targets. Probability of a target report is constant throughout the flight, $c = 100$, $\alpha = 5$ [1/distance^2], $\sigma^2 = 0.25$ [distance^2], and $R = 5$ [distance].

Like the scenario with one uniformly-distributed target, the function for P_{TA} has one peak and never crosses the line where $P_{TA} = P_{TR}$. However, as a result of the changing ratio of targets to false targets, the function for P_{FTA} is not necessarily increasing. Figure 10

shows P_{FTA} increases, then decreases, then increases again. For values of P_{FTA} above the local minimum at $P_{FTA} = 0.385$, the unconstrained solution is used. On a plot of P_{TR}^* versus $P_{FTA_{max}}$, a discontinuous jump appears as shown in Figure 11.
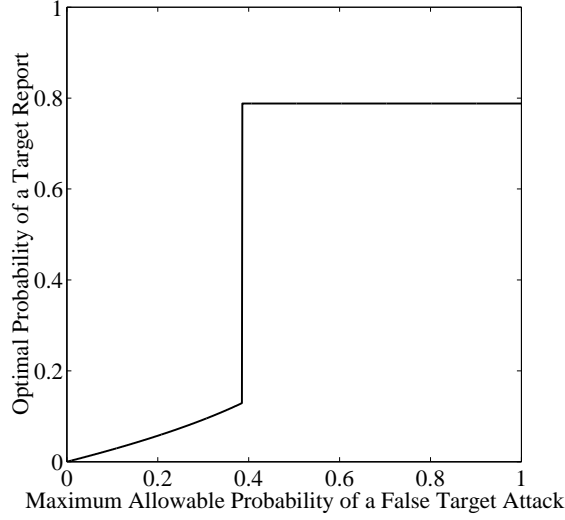
Figure 11. Optimal probability of a target report versus maximum allowable probability of a false target attack. The scenario involves a normally-distributed target and a Poisson field of false targets. Probability of a target report is constant throughout the flight, $c = 100$, $\alpha = 5$ [1/distance^2], $\sigma^2 = 0.25$ [distance^2], and $R = 5$ [distance].

B. Dynamic-Threshold

When P_{TR}, and consequently P_{FTR}, are dynamic, the state variables become

$$x = \int_0^r 2\pi\alpha\rho \left[1 - P_{FTR}(\rho)\right] d\rho \tag{55}$$

$$y = \int_0^r P_{TR}(\rho) \frac{\rho}{\sigma^2} e^{-\frac{\rho^2}{2\sigma^2}} d\rho \tag{56}$$

$$z = \int_0^r 2\pi\alpha\rho \left[1 - P_{FTR}(\rho)\right]\left[1 - y(\rho)\right] e^{-x(\rho)} d\rho \tag{57}$$

and L is

$$L = -P_{TR}(r) \frac{r}{\sigma^2} e^{-\frac{r^2}{2\sigma^2}} e^{-x(r)}. \tag{58}$$

The state equations are

$$\dot{x} = 2\pi\alpha r \left[1 - P_{FTR}(r)\right] \tag{59}$$

$$\dot{y} = P_{TR}(r) \frac{r}{\sigma^2} e^{-\frac{r^2}{2\sigma^2}} \tag{60}$$

$$\dot{z} = 2\pi\alpha r \left[1 - P_{FTR}(r)\right]\left[1 - y(r)\right] e^{-x(r)} \tag{61}$$

After applying Eq. (1) for the ROC model, the Hamiltonian becomes

$$H = \left(\lambda_y - e^{-x}\right) P_{TR}(r) \frac{r}{\sigma^2} e^{-\frac{r^2}{2\sigma^2}} + 2\pi\alpha r \frac{P_{TR}}{(1-c)P_{TR}+c} \left[\lambda_x + \lambda_z (1-y) e^{-x}\right] \quad (62)$$

and the costate differential equations become

$$\dot{\lambda}_x = \lambda_z 2\pi\alpha r \frac{P_{TR}}{(1-c)P_{TR}+c}(1-y)e^{-x} - P_{TR}(r)\frac{r}{\sigma^2}e^{-\frac{r^2}{2\sigma^2}}e^{-x} \quad (63)$$

$$\dot{\lambda}_y = \lambda_z 2\pi\alpha r \frac{P_{TR}}{(1-c)P_{TR}+c}e^{-x} \quad (64)$$

$$\dot{\lambda}_z = 0 \quad (65)$$

Taking the partial derivative of H with respect to the decision variable P_{TR} gives

$$\frac{\partial H}{\partial P_{TR}} = \left(\lambda_y - e^{-x}\right)\frac{r}{\sigma^2}e^{-\frac{r^2}{2\sigma^2}} + \frac{\left[\lambda_x + \lambda_z (1-y)e^{-x}\right]2\pi\alpha rc}{\left[(1-c)P_{TR}+c\right]^2} \quad (66)$$

Solving $\frac{\partial H}{\partial P_{TR}} = 0$, the optimal control is

$$P_{TR}^*(r) = \frac{c \pm \sqrt{\frac{\left[\lambda_x(r)+\lambda_z[1-y(r)]e^{-x(r)}\right]2\pi\alpha c\sigma^2 e^{\frac{r^2}{2\sigma^2}}}{\left[e^{-x(r)}-\lambda_y(r)\right]}}}{c-1}. \quad (67)$$

Once again, only the "minus" root is used. One is also interested in the optimal unconstrained solution, which is

$$P_{TR_u}^*(r) = \frac{c - \sqrt{\lambda_x(r)\,2\pi\alpha c\sigma^2 e^{\left[x(r)+\frac{r^2}{2\sigma^2}\right]}}}{c-1}. \quad (68)$$

Taking the derivative of Eq. (68) with respect to r gives

$$\dot{P}_{TR_u}^*(r) = -\sqrt{\frac{2\pi\alpha c r^2}{4(c-1)^2\sigma^2\lambda_x(r)e^{\left[x(r)+\frac{r^2}{2\sigma^2}\right]}}}\left\{\lambda_x(r)\,e^{\left[x(r)+\frac{r^2}{2\sigma^2}\right]} - \frac{(c-1)}{c}\left[P_{TR}^*(r)\right]^2\right\}. \quad (69)$$

Unlike the previous scenarios, it is unclear whether $P_{TR_u}^*$ is increasing or decreasing.

Assuming $c = 100$, $\alpha = 5$ [1/distance^2], $\sigma^2 = 0.25$ [distance^2], and $R = 5$ [distance], the constrained problem is solved for a number of $P_{FTA_{max}}$ values. Figure 12 shows as $P_{FTA_{max}}$ decreases, the sensor is "turned off" earlier in the search.
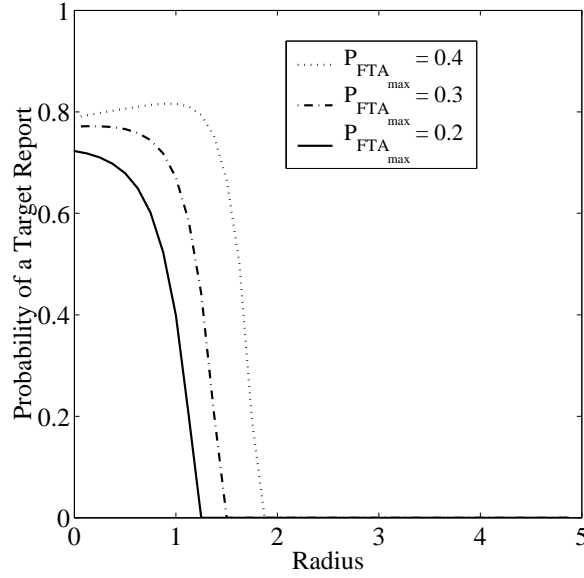
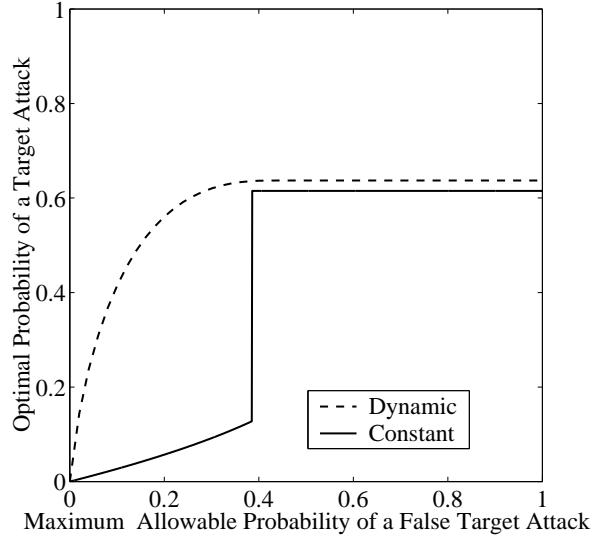**Figure 12.** Optimal probability of a target report versus radius. The scenario involves a normally-distributed target and a Poisson field of false targets. $c = 100$, $\alpha = 5$ $[\mathbf{1/distance^2}]$, $\sigma^2 = 0.25$ $[\mathbf{distance^2}]$, and $R = 5$ $[\mathbf{distance}]$.

The objective function values of the dynamic solutions are compared to those of the constant solutions. Figure 13 shows the poor performance of the constant-threshold solution when $P_{FTA_{max}} < 0.385$. Unlike the previous two scenarios where dynamic-threshold solutions were only a few percent better than constant-threshold solutions, there is substantial improvements when $P_{FTA_{max}} < 0.385$. Since the dynamic problem allows the sensor to be "turned off" at some point, the solutions are similar to those at smaller R values. In essence, one learns how far out in radius to search. The dynamic problem "recognizes" the benefit of staying close to the origin when a target is normally distributed. The constant-parameter problem forces one to arbitrarily pick R then optimize P_{TR} based on R. Thus, one must settle for poor performance when R is chosen too large.

Figure 13. Optimal probability of a target attack versus maximum allowable probability of a false target attack. The scenario involves a normally-distributed target and a Poisson field of false targets. $c = 100$, $\alpha = 5$ **[1/distance^2],** $\sigma^2 = 0.25$ **[distance^2], and** $R = 5$ **[distance].**

V. Conclusion

Three scenarios were considered involving an airborne munition searching for stationary targets among a field of false targets. Targets were modelled using uniform, Poisson, and normal distributions. False targets were modelled using Poisson distributions. The control variable was the probability of a target report, which is linked to the probability of a false target report via the sensor's Receiver Operating Characteristic curve. Optimization problems were formulated that maximize the probability of a target attack while at the same time constraining the probability of a false target attack. Generalized expressions for these two probabilities were derived for all three scenarios. Both constant and dynamic-threshold solutions were given for a sample instance of each scenario. For the two scenarios involving constant target to false target ratios, the optimal dynamic threshold was only a few percent better than the best constant threshold. For the scenario where target to false target ratio changed during the search, the optimal dynamic threshold was substantially better than the optimal constant threshold.

Future work will include parameterizing Receiver Operating Characteristic curves by area coverage rate and formulating problems for air vehicles with multiple warheads. These generalizations will open the solution space to planar regions and expand the applications to unmanned combat air vehicles and general sensor craft. As autonomous unmanned vehicles become more and more prevalent in combat environments, more basic research involving analytic effectiveness measures (like the work presented here) is needed.

Appendix

Formulae for probabilities of events are derived when parameters vary with time or space. Specifically, one is interested in the probability of no target attacks and the probability of no false target attacks prior to a time t or radius r. For example, no target attacks happen if no targets were encountered or all targets encountered were misclassified. One can denote by P_c a general classification probability which can assume the role of P_{TR}, $1 - P_{TR}$, P_{FTR}, or $1 - P_{FTR}$ depending on the application. Events involving only encounters are denoted $\mathcal{E}$, and events involving classified encounters are denoted $\mathcal{C}$. The number of events occurring in a given area is subscripted along with the applicable area. For example, 1 classified encounter in ΔA_1 is denoted $\mathcal{C}_{1,\Delta A_1}$.

A.   Uniform Distribution

Consider the case of searching for one uniformly-distributed target. The air vehicle flies a straight path as illustrated in Figure 1(a); however, its classification probabilities, search width, and velocity are allowed to vary with time. The probability of no encounters (and hence no classification) during $[0, t]$ is

$$P\left(\mathcal{E}_{0,A}\right) = 1 - \frac{1}{A_s} \int_0^t w\left(\tau\right) v\left(\tau\right) d\tau \tag{70}$$

where

$$A_s = \int_0^T w\left(\tau\right) v\left(\tau\right) d\tau. \tag{71}$$

To calculate the probability of exactly one classified encounter occurring during $[0, t]$, divide the time interval into n short time periods of length $\tau_1, \ldots, \tau_n$ such that

$$\sum_{i=1}^n \tau_i = t \tag{72}$$

Let the mean probability of classification, search width, and velocity in the ith interval be P_{c_i}, w_i, and v_i respectively. The incremental area is given by

$$\Delta A_i = w_i v_i \tau_i \tag{73}$$

and the search area is given

$$A_s = \sum_i^n \Delta A_i. \tag{74}$$

The probability of exactly one classified encounter occurring during $[0, t]$ requires considering all the permutations where one classified encounter could occur. That is

$$P\left(\mathcal{C}_{1,A}\right) = P\left(\mathcal{C}_{1,\Delta A_1}\right) + P\left(\mathcal{C}_{1,\Delta A_2}\right) + \cdots + P\left(\mathcal{C}_{1,\Delta A_n}\right) \tag{75}$$

so

$$P\left(\mathcal{C}_{1,A}\right) = \frac{w_1 v_1 \tau_1}{A_s} P_{c_1} + \frac{w_2 v_2 \tau_2}{A_s} P_{c_2} + \cdots + \frac{w_n v_n \tau_n}{A_s} P_{c_n} = \frac{1}{A_s} \sum_{i=1}^{n} w_i v_i \tau_i P_{c_i}. \tag{76}$$

Taking the limit as $\tau_i \to 0$, $i = 1, \ldots, n$, $n \to \infty$ such that $\sum_{i=1}^{n} \tau_i = t$ gives

$$P\left(\mathcal{C}_{1,A}\right) = \frac{1}{A_s} \int_0^t P_c\left(\tau\right) w\left(\tau\right) v\left(\tau\right) d\tau. \tag{77}$$

Now calculate the joint probability of no encounters and one classified encounter during $[0, t]$. The two events are mutually exclusive, thus one must sum the two individual probabilities

$$
\begin{aligned}
P\left(\mathcal{E}_{0,A} \cap \mathcal{C}_{1,A}\right) &= 1 - \frac{1}{A_s} \int_0^t w\left(\tau\right) v\left(\tau\right) d\tau + \frac{1}{A_s} \int_0^t P_c\left(\tau\right) w\left(\tau\right) v\left(\tau\right) d\tau \\
&= 1 - \frac{1}{A_s} \int_0^t \left[1 - P_c\left(\tau\right)\right] w\left(\tau\right) v\left(\tau\right) d\tau.
\end{aligned}
\tag{78}
$$

For the probability of no target attack prior to time t, Eq. (78) is used with $P_c\left(\tau\right) = 1 - P_{TR}\left(\tau\right)$ giving

$$P_{\overline{TA}}\left(t\right) = 1 - \frac{1}{A_s} \int_0^t P_{TR}\left(\tau\right) w\left(\tau\right) v\left(\tau\right) d\tau \tag{79}$$

B.   Poisson Distribution

Let $\mu\left(\tau\right)$ be the rate of encounters at time τ. Divide the time interval $[0, t]$ into n short time periods of length $\tau_1, \ldots, \tau_n$ such that

$$\sum_{i=1}^{n} \tau_i = t \tag{80}$$

Let the mean rate of occurrence and mean probability of classification in the ith interval be μ_i and P_{c_i} respectively. The standard Poisson probability law requires, "If an area is subdivided into n subareas and for $i = 1, \ldots, n$, E_i denotes the event that at least one or more encounters occur in the ith subarea, then, for any integer n, $E_1, \ldots, E_n$ are independent events."[3] Hence,

the probability that exactly j_i encounters occur in the interval τ_i, $i = 1, \ldots, n$ is

$$
\begin{aligned}
P(j_1, \ldots, j_n) &= \prod_{i=1}^{n} e^{-\mu_i \tau_i} \frac{(\mu_i \tau_i)^{j_i}}{j_i!} \\
&= e^{-\sum_{i=1}^{n} \mu_i \tau_i} \prod_{i=1}^{n} \frac{(\mu_i \tau_i)^{j_i}}{j_i!}
\end{aligned}
\tag{81}
$$

The probability of no encounters occurring (and hence no classification) during $[0, t]$ is

$$
P(\mathcal{E}_{0,A}) = e^{-\sum_{i=1}^{n} \mu_i \tau_i}
\tag{82}
$$

Let $j = 1$. The probability of one classified encounter in the ith interval is

$$
P(\mathcal{C}_{1,\Delta A_i}) = e^{-\sum_{i=1}^{n} \mu_i \tau_i} \frac{(\mu_i \tau_i)^{1}}{1!} P_{c_i}.
\tag{83}
$$

The probability of exactly one classified encounter occurring during $[0, t]$ requires considering all the permutations where one classified encounter could occur. That is

$$
P(\mathcal{C}_{1,A}) = P(\mathcal{C}_{1,\Delta A_1}) + P(\mathcal{C}_{1,\Delta A_2}) + \cdots + P(\mathcal{C}_{1,\Delta A_n})
\tag{84}
$$

So,

$$
\begin{aligned}
P(\mathcal{C}_{1,A}) &= e^{-\sum_{i=1}^{n} \mu_i \tau_i} \frac{(\mu_1 \tau_1)^{1}}{1!} P_{c_1} + e^{-\sum_{i=1}^{n} \mu_i \tau_i} \frac{(\mu_2 \tau_2)^{1}}{1!} P_{c_2} + \cdots + e^{-\sum_{i=1}^{n} \mu_i \tau_i} \frac{(\mu_n \tau_n)^{1}}{1!} P_{c_n} \\
&= e^{-\sum_{i=1}^{n} \mu_i \tau_i} \sum_{i=1}^{n} \mu_i \tau_i P_{c_i}
\end{aligned}
\tag{85}
$$

The probability of exactly two classified encounters occurring during $[0, t]$ requires considering all the permutations where two classified encounters could occur. That is

$$
\begin{aligned}
P(\mathcal{C}_{2,A}) &= P(\mathcal{C}_{1,\Delta A_1} \cap \mathcal{C}_{1,\Delta A_2}) + P(\mathcal{C}_{1,\Delta A_1} \cap \mathcal{C}_{1,\Delta A_3}) + \cdots + P(\mathcal{C}_{1,\Delta A_1} \cap \mathcal{C}_{1,\Delta A_n}) + \\
&\quad P(\mathcal{C}_{1,\Delta A_2} \cap \mathcal{C}_{1,\Delta A_3}) + P(\mathcal{C}_{1,\Delta A_2} \cap \mathcal{C}_{1,\Delta A_4}) + \cdots + P(\mathcal{C}_{1,\Delta A_2} \cap \mathcal{C}_{1,\Delta A_n}) + \\
&\quad \vdots \\
&\quad + P(\mathcal{C}_{1,\Delta A_{n-1}} \cap \mathcal{C}_{1,\Delta A_n}) + \\
&\quad P(\mathcal{C}_{2,\Delta A_1}) + P(\mathcal{C}_{2,\Delta A_2}) + \cdots + P(\mathcal{C}_{2,\Delta A_n})
\end{aligned}
\tag{86}
$$

So,

$$
\begin{aligned}
P\left(\mathcal{C}_{2,A}\right) & = e^{-\sum_{i=1}^{n}\mu_i\tau_i}\frac{(\mu_1\tau_1)^1}{1!}P_{c_1}\left[\frac{(\mu_2\tau_2)^1}{1!}P_{c_2}+\cdots+\frac{(\mu_n\tau_n)^1}{1!}P_{c_n}\right]+ \\
& \quad e^{-\sum_{i=1}^{n}\mu_i\tau_i}\frac{(\mu_2\tau_2)^1}{1!}P_{c_2}\left[\frac{(\mu_3\tau_3)^1}{1!}P_{c_3}+\cdots+\frac{(\mu_n\tau_n)^1}{1!}P_{c_n}\right]+ \\
& \quad \vdots \\
& \quad e^{-\sum_{i=1}^{n}\mu_i\tau_i}\frac{(\mu_{n-1}\tau_{n-1})^1}{1!}P_{c_{n-1}}\frac{(\mu_n\tau_n)^1}{1!}P_{c_n}+ \\
& \quad e^{-\sum_{i=1}^{n}\mu_i\tau_i}\left[\frac{(\mu_1\tau_1)^2}{2!}P_{c_1}^2+\cdots+\frac{(\mu_n\tau_n)^2}{2!}P_{c_n}^2\right] \\
& = \frac{1}{2}e^{-\sum_{i=1}^{n}\mu_i\tau_i}\left[2\mu_1\tau_1 P_{c_1}\left(\mu_2\tau_2 P_{c_2}+\cdots+\mu_n\tau_n P_{c_n}\right)+\right. \\
& \quad 2\mu_2\tau_2 P_{c_2}\left(\mu_3\tau_3 P_{c_3}+\cdots+\mu_n\tau_n P_{c_n}\right)+ \\
& \quad \cdots+2\mu_{n-1}\tau_{n-1}P_{c_{n-1}}\mu_n\tau_n P_{c_n}+ \\
& \quad \left. \left(\mu_1\tau_1 P_{c_1}\right)^2+\left(\mu_2\tau_2 P_{c_2}\right)^2+\cdots+\left(\mu_n\tau_n P_{c_n}\right)^2\right] \\
& = e^{-\sum_{i=1}^{n}\mu_i\tau_i}\frac{\left(\sum_{i=1}^{n}\mu_i\tau_i P_{c_i}\right)^2}{2} \qquad (87)
\end{aligned}
$$

In general, the probability of exactly j classified encounters occurring during $[0,t]$ is

$$
P\left(\mathcal{C}_{j,A}\right) = e^{-\sum_{i=1}^{n}\mu_i\tau_i}\frac{\left(\sum_{i=1}^{n}\mu_i\tau_i P_{c_i}\right)^j}{j!} \qquad (88)
$$

Taking the limit as $\tau_i \to 0$, $i = 1,\ldots,n$, $n \to \infty$ such that $\sum_{i=1}^{n}\tau_i = t$ yields

$$
P\left(\mathcal{C}_{j,A}\right) = e^{-\int_0^t \mu(\tau)d\tau}\frac{\left(\int_0^t P_c(\tau)\mu(\tau)\,d\tau\right)^j}{j!} \qquad (89)
$$

Equation (89) can be used to determine the probability of either no false target attacks or no target attacks occurring up through time t. In the case of no false target attacks, the possible mutually exclusive events are

no encounters

1 encounter correctly classified

2 encounters correctly classified

$\vdots$

∞ encounters correctly classified

Thus,

$$
\begin{aligned}
P\left(\mathcal{E}_{0,A} \cap \mathcal{C}_{1,A} \cap \ldots \cap \mathcal{C}_{\infty,A}\right) &= P\left(\mathcal{E}_{0,A}\right) + P\left(\mathcal{C}_{1,A}\right) + \cdots + P\left(\mathcal{C}_{\infty,A}\right) \\
&= e^{-\int_0^t \mu(\tau)d\tau} + e^{-\int_0^t \mu(\tau)d\tau} \frac{\left(\int_0^t P_c(\tau)\mu(\tau)d\tau\right)^1}{1!} + \\
&\quad \cdots + e^{-\int_0^t \mu(\tau)d\tau} \frac{\left(\int_0^t P_c(\tau)\mu(\tau)d\tau\right)^\infty}{\infty!} \\
&= e^{-\int_0^t \mu(\tau)d\tau} \left[1 + \frac{\left(\int_0^t P_c(\tau)\mu(\tau)d\tau\right)^1}{1!} + \cdots + \frac{\left(\int_0^t P_c(\tau)\mu(\tau)d\tau\right)^\infty}{\infty!}\right] \\
&= e^{-\int_0^t \mu(\tau)d\tau} e^{\int_0^t P_c(\tau)\mu(\tau)d\tau} \\
&= e^{-\int_0^t [1 - P_c(\tau)]\mu(\tau)d\tau} \quad\quad (90)
\end{aligned}
$$

To calculate the probability of no false target attacks, let $P_c(\tau) = P_{FTR}(\tau)$ and $\mu(\tau) = \alpha(\tau)w(\tau)v(\tau)$ in Eq. (90) giving

$$
P_{\overline{FTA}}(t) = e^{-\int_0^t [1 - P_{FTR}(\tau)]\alpha(\tau)w(\tau)v(\tau)d\tau} \quad\quad (91)
$$

where $\alpha(\tau)$ is the false target density. To calculate the probability of no target attacks, let $P_c(\tau) = 1 - P_{TR}(\tau)$ and $\mu(\tau) = \beta(\tau)w(\tau)v(\tau)$ in Eq. (90) giving

$$
P_{\overline{TA}}(t) = e^{-\int_0^t [P_{TR}(\tau)]\beta(\tau)w(\tau)v(\tau)d\tau} \qu\quad (92)
$$

where $\beta(\tau)$ is the target density. The integrals in Eq. (91) and Eq. (92) serve as Poisson parameters, which are assumed constant in the literature. These integrals are "dynamic Poisson parameters". When formulating optimal control problems, states are used to represent the integrals.

C.   Normal Distribution

Consider the case of searching for one normally-distributed target in a circular disc of radius r. Normally-distributed refers to circular normal distribution with standard deviation σ. The classification probabilities vary with radius. The probability of no encounters (and hence no classification) searching a disc of radius r from the origin outward using concentric annuli of thickness $d\rho$ is

$$
P\left(\mathcal{E}_{0,A}\right) = 1 - \int_0^{2\pi} \int_0^r \frac{1}{2\pi\sigma^2} e^{-\frac{\rho^2}{2\sigma^2}} \rho\, d\rho\, d\theta = 1 - \int_0^r \frac{1}{\sigma^2} e^{-\frac{\rho^2}{2\sigma^2}} \rho\, d\rho. \quad\quad (93)
$$

To calculate the probability of one classified encounter, divide the disc of area A into n concentric annuli of area $A_1, \ldots, A_n$ such that

$$\sum_{i=1}^{n} A_i = A \tag{94}$$

Each A_i is calculated using

$$A_i = 2\pi \rho_i \Delta \rho_i \tag{95}$$

where ρ_i is the radius of the annulus and $\Delta \rho_i$ is the thickness. The search begins at the origin of the disc and progresses outward such that $\rho_i < \rho_{i+1}$, $i = 1, \ldots, n-1$. Let the mean probability of classification in the ith annulus be P_{c_i}. The probability of one classified encounter during the sweep of A requires considering all the permutations where one classified encounter could occur. That is

$$P\left(\mathcal{C}_{1,A}\right) = P\left(\mathcal{C}_{1,\Delta A_1}\right) + P\left(\mathcal{C}_{1,\Delta A_2}\right) + \cdots + P\left(\mathcal{C}_{1,\Delta A_n}\right) \tag{96}$$

so

$$P\left(\mathcal{C}_{1,A}\right) = 2\pi \rho_1 \Delta \rho_1 \frac{1}{2\pi\sigma^2} e^{-\frac{\rho_1^2}{2\sigma^2}} P_{c_1} + \cdots + 2\pi \rho_n \Delta \rho_n \frac{1}{2\pi\sigma^2} e^{-\frac{\rho_n^2}{2\sigma^2}} P_{c_n} = \sum_{i=1}^{n} \frac{1}{\sigma^2} \rho_i \Delta \rho_i e^{-\frac{\rho_i^2}{2\sigma^2}} P_{c_i}. \tag{97}$$

Taking the limit as $\Delta \rho_i \to 0$, $i = 1, \ldots, n$, $n \to \infty$ such that $\sum_{i=1}^{n} A_i = A$ yields

$$P\left(\mathcal{C}_{1,A}\right) = \int_0^r \frac{P_c\left(\rho\right)}{\sigma^2} e^{-\frac{\rho^2}{2\sigma^2}} \rho d\rho. \tag{98}$$

Now calculate the joint probability of no encounters and one classified encounter during the sweep of A. The two events are mutually exclusive, thus one must sum the two individual probabilities

$$
\begin{aligned}
P\left(\mathcal{E}_{0,A} \cap \mathcal{C}_{1,A}\right) &= 1 - \int_0^r \frac{1}{\sigma^2} e^{-\frac{\rho^2}{2\sigma^2}} \rho d\rho + \int_0^r \frac{P_c\left(\rho\right)}{\sigma^2} e^{-\frac{\rho^2}{2\sigma^2}} \rho d\rho \\
&= 1 - \int_0^r \frac{\left[1 - P_c\left(\rho\right)\right]}{\sigma^2} e^{-\frac{\rho^2}{2\sigma^2}} \rho d\rho.
\end{aligned} \tag{99}
$$

For the probability of no target attack prior to radius r, Eq. (99) is used with $P_c\left(\rho\right) = 1 - P_{TR}\left(\rho\right)$ giving

$$P_{\overline{TA}}\left(r\right) = 1 - \int_0^r \frac{P_{TR}\left(\rho\right)}{\sigma^2} e^{-\frac{\rho^2}{2\sigma^2}} \rho d\rho \tag{100}$$

References

[1] Koopman, B.O., *Search and Screening*, Pergamon Press, Inc., 1980.

[2] Washburn, A.R., *Search and Detection*, Operations Research Society of America, 1981.

[3] Jacques, D.R. and Pachter, M., "A Theoretical Foundation for Cooperative Search, Classification, and Target Attack", *Cooperative Control: Models, Applications and Algorithms*, Kluwer Academic Publishers, 2004.

[4] Moses, L.E., Shapiro, D.E. and Littenberg, B., "Combining Independent Studies of a Diagnostic Test into a Summary ROC Curve: Data-analytic Approaches and Some Additional Considerations, *Statistics in Medicine, Vol. 12*, John Wiley and Sons, Ltd., 1993.

[5] Bryson, A.E. and Ho, Y., *Applied Optimal Control*, Ginn and Company, 1969.

[6] Bryson, A.E., *Dynamic Optimization*, Addison-Wesley, 1999.